

Pulsed Plasma Polymerization of Benzaldehyde for Retention of the Aldehyde Functional Group

Megan A. Leich,[†] Neil M. Mackie, Keri L. Williams, and Ellen R. Fisher*

Department of Chemistry, Colorado State University, Fort Collins, Colorado 80523-1872

Received March 3, 1998; Revised Manuscript Received September 9, 1998

ABSTRACT: Pulsed plasma polymerization of benzaldehyde is used to produce thin films containing aldehyde functional groups. The effects of pulse peak power, pulse-on time, duty cycle, and monomer pressure on film composition, especially aldehyde functional groups, and surface polarity are examined. Film properties are determined using Fourier transform infrared (FTIR) spectroscopy, X-ray photoelectron spectroscopy (XPS), contact angle measurements, and scanning electron microscopy (SEM). Analysis using these techniques shows retention of the aromatic structure occurs with the longest off times and smallest duty cycles while retention of the aldehyde group occurs only under plasma conditions that result in fragmentation of the aromatic ring, higher peak pulse power, and a relatively large duty cycle (20%).

Introduction

Pulsed rf power has been successfully employed in the plasma polymerization of a variety of monomers.^{1,2} With pulsed plasma polymerization, high retention of the monomer functional group in the resulting polymeric film can be achieved.³ This is in stark contrast to results for films deposited from continuous (CW) plasmas, where deposited films are often amorphous polymeric materials whose structures bear little resemblance to that of the original monomer.^{4,5} One reason for these differences is that pulsed plasmas provide access to lower CW equivalent powers because the rf power is only on for a portion of the cycle time. In addition CW plasmas can significantly fragment and scramble monomer functional groups through complex recombination and addition reactions.⁶ Use of pulsed sources reduces trapped radicals in the film, lowers deposition surface temperatures, decreases high-energy ion bombardment and UV flux to the surface, and provides greater control over the resulting film chemistry.⁷ We have previously reported the use of pulsed rf plasmas to produce a variety of organic films with a high degree of controllability over film composition.^{3,5} Additional work in this area has concentrated on inorganic materials such as amorphous hydrogenated silicon carbide ($\text{a-Si}_{1-x}\text{C}_x\text{H}$).^{8,10}

In the present work, benzaldehyde is used as the monomer in a series of pulsed plasma polymerizations. The main goal is to explore pulsed plasma conditions that result in retention of the aldehyde functional group on the surface of the deposited polymeric film.⁹ Zhao et al. have performed CW plasma polymerization using benzaldehyde but found little retention of the aldehyde functional group in their films using infrared spectroscopy, thermogravimetric analysis, contact angle goniometry, and gas chromatography–mass spectrometry (GC-MS).^{10,11} Instead, an abundance of ketone functional groups was observed, suggesting that the terminal hydrogen of the aldehyde group was extremely labile during plasma polymerization. This seems reasonable,

as the C–H bond on the aldehyde group is the weakest bond in the monomer ($D_0 \sim 78$ kcal/mol).¹² Griesser and co-workers have also explored CW plasma polymerization of aldehyde monomers using very low applied power (5 W) and low-frequency (125–375 kHz) rf plasmas.⁹ They observed that retention of aldehyde functionality was both monomer dependent and frequency dependent, with lower frequencies yielding greater retention of polar groups. Pulsed plasma polymerization offers an alternate route to aldehyde retention through gentler fragmentation pathways. Retention of the aldehyde groups offers the possibility of further functionalizing the polymer film through traditional aldehyde reduction reactions. Moreover, if the aldehyde moieties are retained in the outermost layers of the deposited film, they could greatly enhance interfacial interactions with additional layers.

Experimental Methods

All films were deposited in our home-built inductively coupled rf plasma reactor, described previously.^{5,13} In these experiments, the applied peak power was varied from 25 to 100 W. The pulse-on time and duty cycle (defined as the ratio of pulse-on time to total cycle time) were varied using the internal pulse generator of an RF Power Products RF5S (13.56 MHz) power supply. For each deposition, a freshly pressed FTIR grade KBr (Aldrich) pellet and a silicon wafer (p-type, 110 with 40–60 Å of native oxide) were used as substrates. These were placed on glass microscope slides oriented parallel to the gas flow in the coil region of the reactor chamber. Pulsed deposition times ranged from 2 to 10 min, as defined by the total time the sample was exposed to both pulse-on and pulse-off cycles.

Benzaldehyde (Aldrich, 99+% purity) was placed in a liquid bulb and underwent several freeze–pump–thaw cycles before use to remove trapped atmospheric gases. Reactant vapor pressure was controlled through a Nupro needle valve, and the total pressure in the reactor was maintained at ~ 25 mTorr above a base pressure of 0–2 mTorr. Transmission FTIR spectra on KBr pellets and Si wafers were collected ex situ using a Nicolet Magna 760 FTIR spectrometer (resolution of 8 cm^{-1} and averaging over 100 scans). Spectra shown are corrected for residual carbon dioxide not purged from the FTIR spectrometer (absorbances at ~ 2340 and 2360 cm^{-1}).

X-ray photoelectron spectroscopy (XPS) experiments were performed on a Surface Science Instruments S-probe spec-

[†] Present Address: Department of Chemistry, University of Oregon, Eugene, OR 97403.

* To whom correspondence should be addressed.

Table 1. FTIR Absorption Assignments

absorbance (cm ⁻¹)	assignment	ref
600–900	out-of-plane deformation of Ph–H	11
700 } 760 }	out-of-plane phenyl ring bending mode	16
1451	in-plane phenyl ring bending mode, CH ₃ bend	16
1633	C=C	16
1675	α,β -unsaturated ketone	11
1680	aromatic ketone	10, 11
1701	benzaldehyde C=O stretch	10, 11
1703	cyclic ketone C=O stretch	11
2737 } 2817 }	benzaldehyde C–H stretch	10, 11
2843–2863	C–H symmetric stretch, methylene	15
2862–2882	C–H symmetric stretch, methyl	15
2916–2936	sp ³ CH ₂ or CH ₃	15
2925	sp ³ CH ₂	15
3025 } 3058 } 3088 }	aromatic sp ² CH stretch	15, 16
3200–3600	O–H stretch, bonded hydroxyl	16

trometer. This system has a monochromatic Al K α X-ray source ($h\nu = 1486.6$ eV), a hemispherical analyzer, and a resistive strip multichannel detector. A low-energy (~ 5 eV) electron gun was used for charge neutralization on the nonconducting samples. The binding energy (BE) scales for the samples were referenced by setting the CH_x peak maxima in the C_{1s} spectra to 285.0 eV. The high-resolution C_{1s} spectra were acquired at an analyzer pass energy of 25 eV and an X-ray spot size of 1000 μm . XPS elemental compositions of samples were obtained using a pass energy of 50 eV and were collected at a nominal photoelectron takeoff angle of 55°.

Quantification of the surface alcohol content was obtained using the trifluoroacetic anhydride (TFAA) derivatization technique.¹⁴ Films were exposed to TFAA vapor for 10 min at a static pressure of 200 mTorr. The chamber was then evacuated to 3 mTorr, and the samples were exposed to pyridine vapor for 2 min at 200 mTorr. After derivatization the samples were sealed in vials, evacuated, and backfilled with argon to prevent further postdeposition oxidation prior to XPS analysis.

Film morphology for materials deposited on silicon substrates was determined using a Philips 505 scanning electron microscope, with an accelerating voltage of 20 kV and a spot size of 20 nm. The films were sputtered with 10 nm of gold prior to SEM analysis. Static contact angles for water were measured using the sessile drop method with a contact angle goniometer (Ramé Hart Model 100). Measurements were taken on both sides of water drops at ambient temperature, 30–40 s after 1 μL drops were applied to the surface and the needle tip was removed from each drop. For each sample, six drops were placed at different locations on the surface of a 1000 Å thick film. Reported contact angles are the average of these measurements for three samples.

Results

FTIR Spectroscopy. Table 1 lists the FTIR absorbance bands observed in our films, along with the literature assignments we have adopted. All FTIR spectra were collected from KBr substrates. Pulse parameter notation is given as the ratio of pulse-on time to pulse-off time. For example, 14/56 corresponds to 14 ms on and 56 ms off, or a 20% duty cycle.

Figure 1 shows an FTIR spectrum of the starting monomer, liquid benzaldehyde. Comparison of plasma-polymerized benzaldehyde films and the benzaldehyde monomer gives a reference point to the subtle shifts in absorbance values in the plasma-deposited films. The primary nature of the monomer is shown by two CH stretching absorptions at 2817 and 2737 cm⁻¹, which are shown in greater detail in the expanded region inset

of Figure 1. The aldehyde carbonyl stretch in benzaldehyde is at 1701 cm⁻¹. Other notable peaks are the sp² CH stretch at 3050 cm⁻¹ and the out-of plane phenyl ring bending modes at 700 and 760 cm⁻¹.

Figure 1 also shows FTIR spectra of films deposited from 14/56 ms (20% duty cycle) pulse sequences with peak pulse powers of 50 and 25 W. These data show the sensitivity and control of the deposition process by the pulsed plasma technique. The film deposited from a peak pulse power of 50 W has contributions from OH and sp³ CH and a strong absorbance at 1701 cm⁻¹, indicative of aldehyde carbonyl bonding. Moreover, the aldehyde C–H stretching band at 2737 cm⁻¹ is shown in the expanded region of Figure 1. When the peak pulse power is decreased to 25 W, the resulting film is clearly different. A new absorbance has appeared in the spectrum at 3050 cm⁻¹, attributed to sp² CH stretching. Note that the intensity of this new peak is equivalent to the intensity of the sp³ CH stretch at 2950 cm⁻¹. The strong carbonyl peak is shifted to 1680 cm⁻¹ due to significant aromatic ketone carbonyl absorption, and an equally intense new peak has grown in at 1606 cm⁻¹, attributed to olefinic C=C bonding.¹⁵ In addition, a strong doublet peak is present at 700 and 750 cm⁻¹, attributed to out-of-plane phenyl ring bending.¹⁶ We have observed this type of aromatic ring retention previously with benzene and fluorinated benzene monomers.³ The broad absorption band from 1400 to 1000 cm⁻¹ seen in the film deposited at 50 W can be assigned to a wide range of absorption species such as multiple C–O vibrations for alcohol, ether, and ester species as well as CH bending modes (Table 1). The present results show that, at a low peak pulse power, retention of the aromatic ring is possible, but no aldehyde functionality has been retained in this film. Conversely, at higher peak pulse power, no aromatic functional groups are retained, but there is a significant retention of aldehyde groups.

To explore the effects of pulse duty cycle on film composition, the pulse-on time was held constant and different pulse-off times were employed with a constant peak power of 50 W. Figure 2 shows FTIR spectra of films deposited from benzaldehyde plasmas with 14/14, 14/56, and 14/266 ms pulse sequences. The film deposited from a 14/14 (50% duty cycle) pulsed plasma shows a contribution from OH at ~ 3400 cm⁻¹,¹⁶ a contribution from sp³ CH at ~ 2950 cm⁻¹, and a complicated group

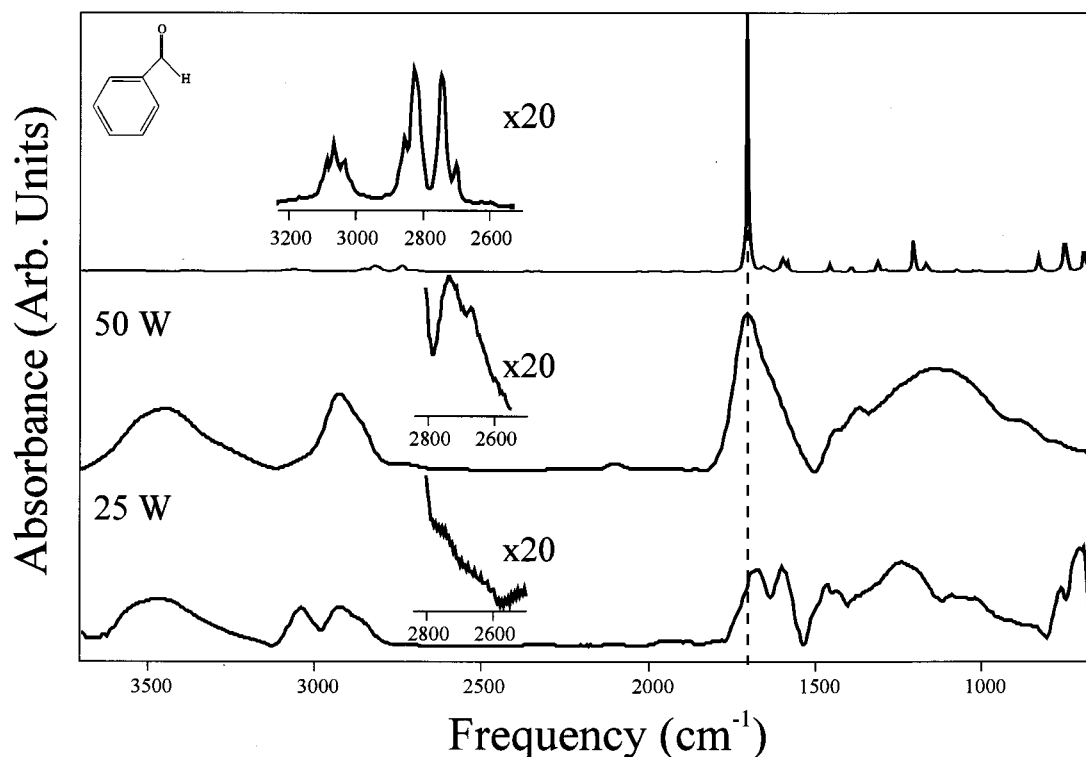


Figure 1. FTIR transmission spectra of liquid benzaldehyde monomer and plasma-polymerized thin films produced from 50 W 14/56 ms and 25 W 14/56 ms pulsed benzaldehyde plasmas. The dashed line indicates the aldehyde carbonyl stretching frequency at 1701 cm^{-1} , and the insets show the aldehyde C-H stretching region from 2600 to 2800 cm^{-1} expanded by a factor of 20.

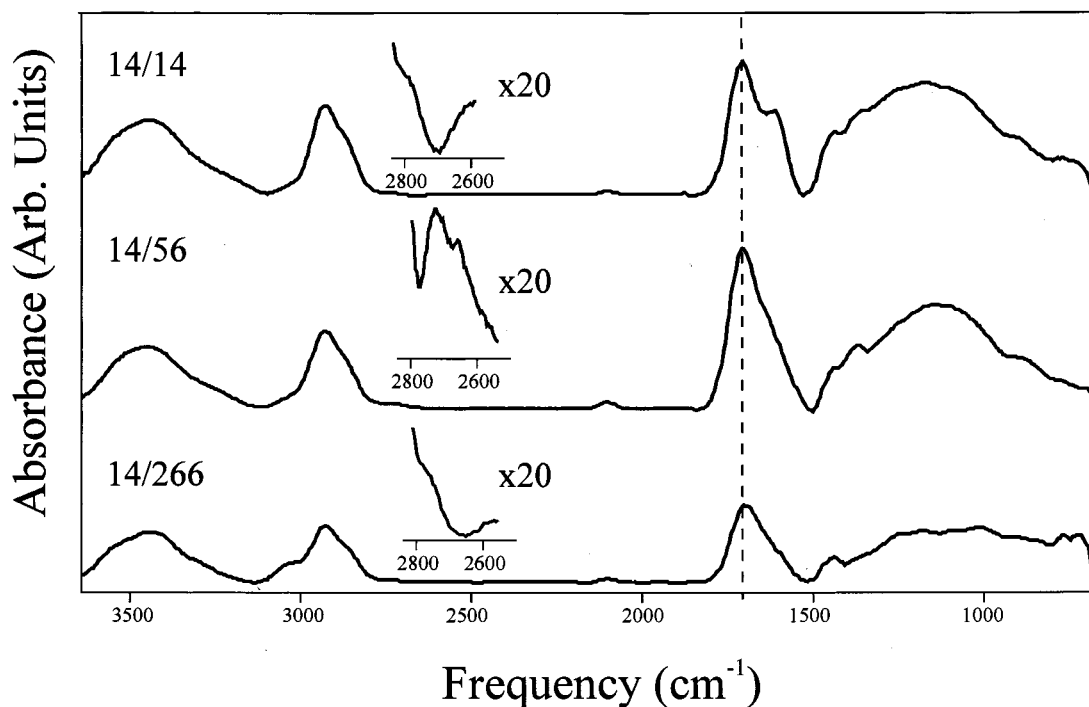


Figure 2. FTIR transmission spectra of films deposited from pulsed benzaldehyde plasmas with 14/14, 14/56, and 14/266 ms pulse sequences at 50 W peak power. The dashed line indicates the aldehyde carbonyl stretching frequency at 1701 cm^{-1} , and the insets show the aldehyde C-H stretching region from 2600 to 2800 cm^{-1} expanded by a factor of 20.

of overlapping absorptions centered around 1700 cm^{-1} . These can be attributed to an aldehyde carbonyl group or a cyclic ketone at 1701 cm^{-1} and an olefinic C=C stretch at 1606 cm^{-1} (Table 1). As noted above, the broad absorption band from 1400 to 1000 cm^{-1} can be assigned to a wide range of absorption species (Table 1).

Increasing the off time to 56 ms (20% duty cycle) yields a film with the same composition shown in Figure 1. When the off time is further increased to 266 ms (5% duty cycle), the CH aldehyde peak disappears and new absorbances at 3050 cm^{-1} (sp^2 CH stretching) and at 754 and 700 cm^{-1} (out-of-plane phenyl ring bending modes) appear.¹⁸ This demonstrates that the phenyl

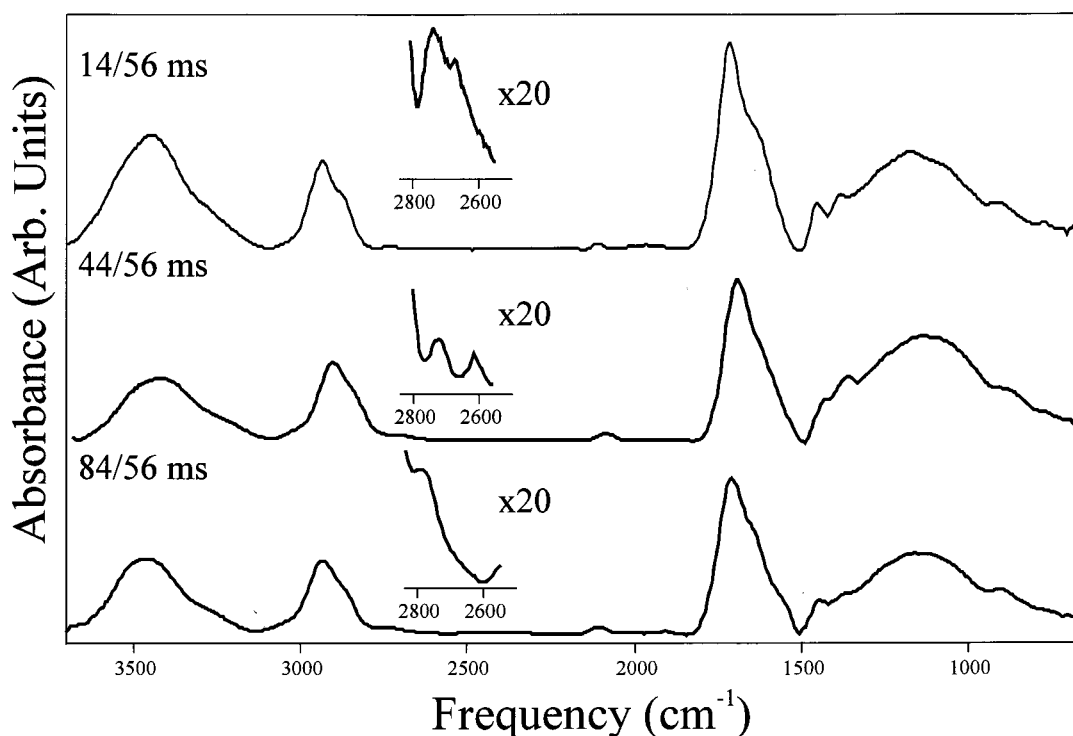


Figure 3. FTIR transmission spectra of films deposited from pulsed benzaldehyde plasmas with 14/14, 44/56, and 84/56 ms pulse sequences at 50 W peak power. The insets show the aldehyde C-H stretching region from 2600 to 2800 cm^{-1} expanded by a factor of 20.

ring from the monomer is retained in the deposited film. The peak of the C=O band has also shifted to below 1701 cm^{-1} , possibly indicating a larger contribution from ketone-like structures in the film, such as aromatic, cyclic, or α,β -unsaturated ketones (Table 1).

We have also explored the effects of keeping the pulse-off time constant and changing the pulse-on time. Figure 3 shows FTIR spectra of films deposited from benzaldehyde plasmas with 14/56, 44/56, and 85/56 ms pulse sequences at 50 W peak power. The spectra for all three films show contributions from OH, sp^3 CH, and carbonyl stretching (Table 1). Film composition is, however, relatively insensitive to pulse-on time, as shown by the similarity of all three spectra. The only significant difference is that there is more aromatic ketone contributions at on times > 14 ms, as indicated by a stronger shoulder on the 1700 cm^{-1} carbonyl peak. Given the results from these two sets of timing sequence experiments, we find that intermediate on times (14 ms) and relatively short off times (56 ms), corresponding to a duty cycle of $\sim 20\%$, yield films with the highest retention of aldehyde groups. On the basis of constant duty cycle experiments (varying on and off times), we find the most important parameter is the length of the off time of the pulse cycle.

The effect of monomer pressure (25, 50, and 100 mTorr) on the resulting composition of the pulsed-plasma-polymerized films is presented in Figure 4. All films were deposited with a pulse sequence of 14/56 ms and 50 W peak power. The film deposited at 25 mTorr shows significant aldehyde CH contributions at 2737 cm^{-1} and a carbonyl peak that is centered at 1707 cm^{-1} . This film also has very small contributions from aromatic functional groups. Increasing the reactor pressure to 50 mTorr increases the sp^2 CH contribution at 3050 cm^{-1} and shifts the carbonyl peak to 1690 cm^{-1} , again indicating an increased contribution of ketone

functional groups. Increasing the pressure to 100 mTorr results in a very different film composition. The carbonyl absorption peak has decreased in intensity, and the olefinic C=C stretch at 1606 cm^{-1} is the dominant absorption in the spectrum. In addition, there is a large increase in the intensity of the out-of-plane phenyl ring stretching modes at 700 and 760 cm^{-1} . This film is very similar in composition to films deposited from 25 W peak pulse power plasmas (Figure 1).

X-ray Photoelectron Spectroscopy. XPS analysis was performed on two sets of films deposited on Si substrates from pulsed benzaldehyde plasmas. The first set of films were deposited with a 14/56 ms pulse cycle and peak rf powers of 25, 50, and 100 W. Surface elemental composition and high-resolution C_{1s} contributions for these films are listed in Table 2. All films contain carbon and oxygen with trace amounts of fluorine.¹⁷ As the peak rf power is increased, there is a progressive increase in the carbon-oxygen bonding relative to carbon-carbon bonding. Table 2 also provides a quantitative measure of the ratio of surface carbon atoms bonded to oxygen atoms obtained from the XPS analyses of the C_{1s} and O_{1s} photoelectron peaks. As these data show, the C/O ratio decreases by a factor of 1.7 as the peak rf power is doubled from 25 to 50 W. However, when the rf power is doubled again to 100 W, the C/O ratio decreases by only a factor of 1.2. A similar trend in C/O ratio is observed with the second set of films, deposited with a peak rf power of 50 W, a constant on time of 14 ms, and off times from 14 to 266 ms. These data indicate that there is significant oxygen retention at moderate rf peak powers and intermediate pulse sequences.

Analysis of the C_{1s} high-resolution spectra for the first set of films shows they contain contributions from C-H (285.0 eV), C-O (286.3 eV), and C=O (287.6 eV) (Table 2). Films deposited at the lowest peak power (25

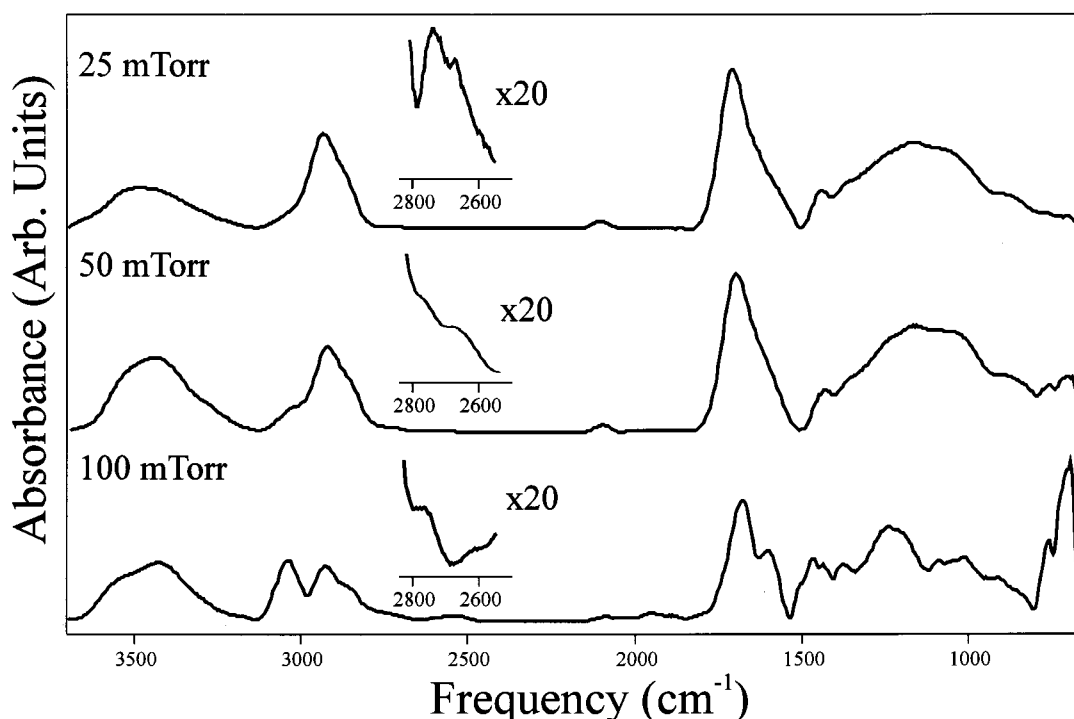


Figure 4. FTIR transmission spectra of films deposited from pulsed benzaldehyde plasmas with operating pressures of 25, 50, and 100 mTorr at a constant pulse sequence of 14/56 and 50 W peak power. The insets show the aldehyde C-H stretching region from 2600 to 2800 cm^{-1} expanded by a factor of 20.

Table 2. Atomic Stoichiometry and $\text{C}_{1\text{s}}$ Contributions for Films Deposited from Benzaldehyde Plasmas^a

applied rf power (W)	pulse on/off (ms)	atom %				stoichiometry ratio ^b	$\text{C}_{1\text{s}}$ contribution %			
		F	O	N	C		CH	C-O	C=O	$\pi-\pi^*$ shake-up
25	14/56	1.4	9.1		89.5	9.8	91	6	2	2
50	14/56	1.3	14.6	1.0	83.2	5.7	81	14	5	
100	14/56	1.1	16.7		82.3	4.9	76	16	9	
50	14/14	0.8	16.0	0.8	82.4	5.2	79	14	6	
50	14/56	1.2	14.1	0.4	84.4	5.9	83	14	5	
50	14/266	1.2	9.4		89.4	9.5	89	8	2	1

^a Taken from high-resolution XPS data. ^b Calculated from the ratio of $\text{C}_{1\text{s}}$ to $\text{O}_{1\text{s}}$ atomic percentages.

W) also exhibit features that are attributed to an aromatic $\pi-\pi^*$ shake-up satellite (291.1 eV). This feature indicates there is aromatic group retention in the deposited film and has been observed previously using low duty cycle pulsed benzene plasmas.³ At higher peak powers (50 W) there is an increase in both the C-O and C=O content in the film and elimination of the aromatic $\pi-\pi^*$ shake-up feature. At the highest peak power (100 W), the C-O contribution does not change, but the C=O contribution is nearly twice that found with the film deposited at 50 W. In the $\text{C}_{1\text{s}}$ spectra of the second set of films, the highest C-O and C=O contributions are found with the shortest off times (14 and 56 ms). At the longest off time (266 ms), the C-O and C=O contributions have decreased by ~50%. However, films deposited at the longest off time also contain a small contribution from the aromatic $\pi-\pi^*$ shake-up feature.

XPS is a powerful and sensitive technique but cannot differentiate between C-O-H and C-O-C or between ketone and aldehyde C=O functional groups due to similarities in their respective binding energies. TFAA derivatization procedures were employed to functionalize surface hydroxyls on our films and thereby discriminate between C-O-H and C-O-C functional groups (Table 3). In this procedure, hydroxyl groups

are converted to OC(O)CF_3 groups via an esterification reaction.¹⁸ Surface hydroxyl content is then determined by observing an increase in fluorine content, and the amount of CF_3 present in the surface of the film. With our films, however, assignment of CF_3 groups is complicated by overlap from $\pi-\pi^*$ shake-up features and the low $\text{C}_{1\text{s}}$ cross section of the CF_3 group. XPS analysis of the TFAA-derivatized samples reveals increases in the F atom % of only 2–3%. This confirms there is very little C-O-H bonding at the surface of all of the deposited films and that the primary singly bonded oxygen is present as ether (C-O-C) functional groups. In contrast, materials deposited from pulsed allyl alcohol plasmas contain considerable amounts of surface alcohol functionalities, as seen by XPS analysis of TFAA-derivatized films.¹⁴ Indeed, films deposited from allyl alcohol plasmas with low duty cycles and relatively long off times contain as much as ~25 atom % fluorine, considerably more than our films (Table 3).

Discrimination between aldehyde and ketone carbonyl groups presents a greater challenge. Griesser and co-workers attempted several aldehyde derivatization techniques for their films deposited from a variety of nonaromatic aldehyde monomers.⁹ These techniques, however, require the use of liquid reagents which are incompatible with the physical properties of the benz-

Table 3. Atomic Stoichiometry and C_{1s} Contributions for Films Derivatized Using TFAA^a

applied rf power (W)	pulse on/off (ms)	atom %				stoichiometry	C _{1s} contribution %				$\pi-\pi^*$
		F	O	N	C	ratio ^b	CH	C—O	C=O	CF ₃	shake-up
						C/O					
25	14/56	1.2	5.9		92.8	15.7	91	4	2		4
50	14/56	3.7	13.6	2.1	80.6	5.9	81	12	8	trace	
100	14/56	3.7	14.9	2.3	79.1	5.3	77	16	8	trace	
50	14/14	3.3	13.4	3.1	80.3	6.0	82	14	4	trace	
50	14/56	3.7	13.6	2.1	80.6	5.9	81	12	8	trace	
50	14/266	2.5	8.0	4.1	85.5	10.7	84	14	2		1

^a Taken from high-resolution XPS data. ^b Calculated from the C_{1s} percentages.

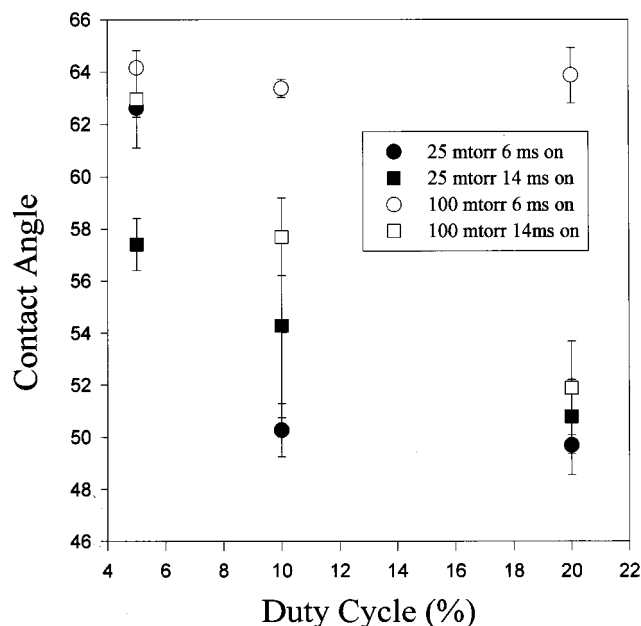


Figure 5. Static contact angles as a function of duty cycle for films deposited from benzaldehyde plasmas with 25 mTorr and 6 ms on times (closed circles), 25 mTorr and 14 ms on times (closed squares), 100 mTorr and 6 ms on times (open circles), and 100 mTorr and 14 ms on times (open squares).

aldehyde films (poor adhesion and hydrophilicity); therefore, attempts at additional aldehyde derivatization techniques were unsuccessful.

Contact Angle. To determine the wettability of film surfaces, static contact angles were measured for films deposited under four different deposition conditions and three different duty cycles (Figure 5).¹⁹ In general, contact angles for the films decrease with increasing duty cycle, indicating a more polar surface is formed at higher duty cycles. The lower pressure (25 mTorr) depositions produce films with the highest surface polarity, while the higher pressure (100 mTorr) deposition films have a more hydrophobic surface. None of the films produced from pulsed plasmas, however, had as high a surface polarity as the films deposited with a CW plasma, $\sim 45^\circ$ at an applied power of 20 W.¹¹ The general trends we observe in contact angle measurements match the FTIR film composition results of Figure 6. The two 25 mTorr depositions display significantly more carbonyl retention than the films deposited at 100 mTorr and show a corresponding low contact angle with water. Additionally, the material deposited at 100 mTorr with a 6 ms on time displays significant aromatic functionality and a reduced carbonyl content. The surface wettability of this film also matches the bulk film composition, as the contact angles across the duty cycles studied are all $\sim 63^\circ$, the highest observed with these materials. Films deposited from

peak pulse powers of 25 W also show increased aromatic content and a significantly higher contact angle of $58 \pm 3^\circ$.

Scanning Electron Microscopy. The morphology of the films was determined using scanning electron microscopy. SEM images for films deposited from pulsed benzaldehyde plasmas show that these films are smooth and pinhole free even at high magnifications. Figure 7 shows a representative sample image of a film deposited from a pulse sequence of 14/56 ms and a peak power of 50 W. As can be seen in this image, the films appear smooth and continuous with no pinholes or defects. All pulse sequences studied here result in films with similar surface morphologies.

Discussion

Timmons and co-workers have examined a wide range of monomers with pulsed plasmas and have observed that the control available over film composition using pulsed plasmas is extremely monomer dependent.^{1,2,7} However, interesting similarities can be found by comparing films produced from pulsed plasmas of benzaldehyde to films produced from pulsed benzene plasmas.^{3,20} Our work on benzene and fluorinated benzene monomers found that polystyrene-like films with some degree of cross-linking were deposited from low-duty-cycle ($\sim 1\%$) plasmas with very short on times and long off times (10/990 pulse sequence).³ XPS data of films deposited from benzene also show contributions to the C_{1s} spectra from the aromatic $\pi-\pi^*$ shake-up satellites under these conditions. Thus, with both benzaldehyde and benzene, maximum retention of aromatic structure occurs with the longest off times and the smallest duty cycles. In addition, aromatic retention with benzaldehyde is also seen using low peak rf powers. These conditions correspond to the lowest plasma power densities. For benzaldehyde, however, these "gentle" plasma conditions also result in little or no aldehyde retention in the deposited film. Retention of aldehyde only occurs under plasma conditions that result in preferential fragmentation of the aromatic ring (Figures 1 and 2 and Table 2).

To understand the processes that are occurring during film deposition from pulsed benzaldehyde plasmas, we need to investigate the relative bond energies of the functional groups of benzaldehyde and the possible fragmentation pathways of the benzaldehyde monomer that can occur. Scheme 1 shows possible reaction pathways for intermediate I after cleavage of the aldehyde CH bond. The viability of Scheme 1 can be explored by consideration of the relative energetics of these gas-phase reactions. Creation of diphenyl ketone by reaction of benzene and benzoyl radicals is a slightly endothermic process, $\Delta H_{rxn} \sim 28$ kcal/mol. The competing decarboxylation reaction is more favorable with

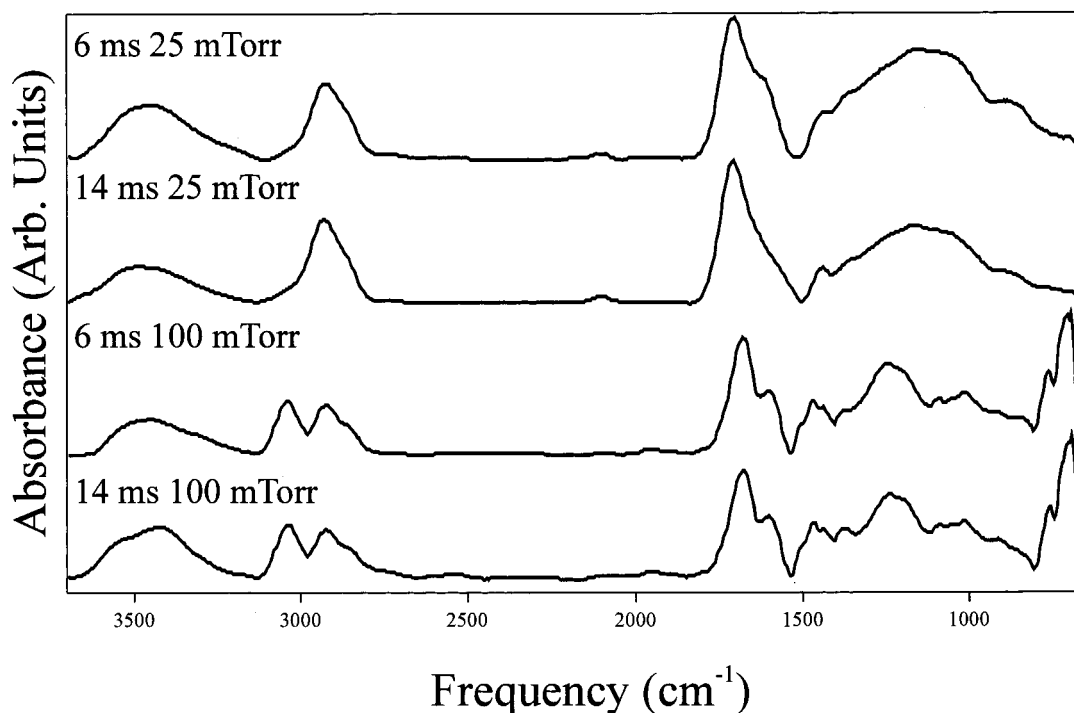


Figure 6. FTIR transmission spectra of films deposited from pulsed benzaldehyde plasmas with on times and operating pressures of 6 ms and 25 mTorr, 14 ms and 25 mTorr, 6 ms and 100 mTorr, and 14 ms and 100 mTorr.

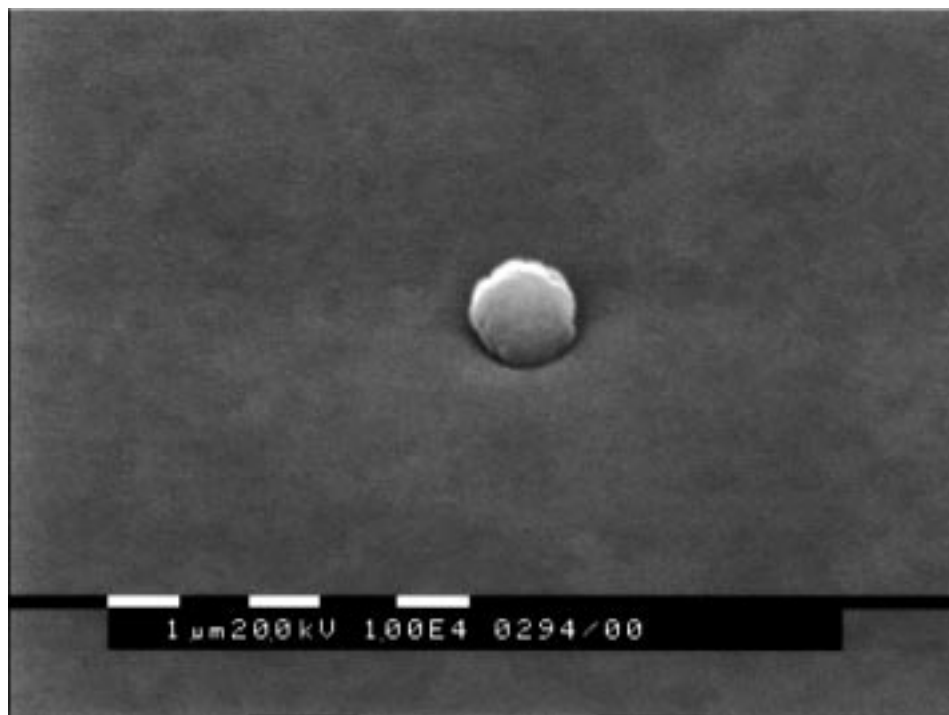
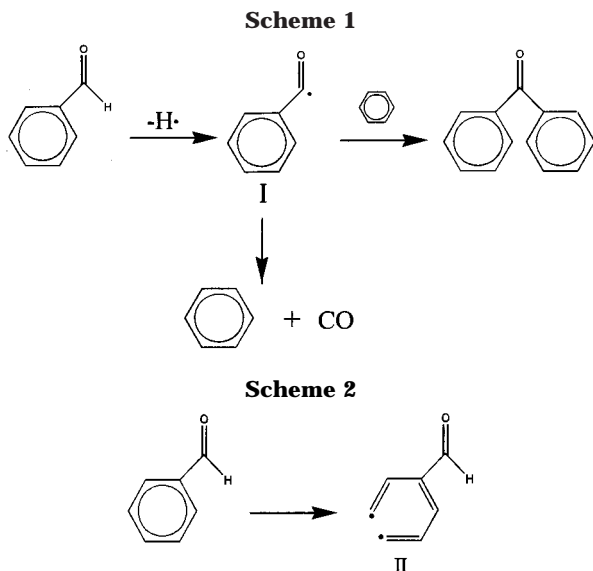


Figure 7. Scanning electron micrograph images ($\times 10\,000$ magnification) of a film deposited from 14/56 ms pulsed benzaldehyde plasmas at 50 W peak applied power and an operating pressure of 25 mTorr.

$\Delta H_{\text{rxn}} \sim -75$ kcal/mol.¹² On the basis of this thermochemistry, the further decomposition of benzaldehyde shown in Scheme 1 is reasonable and accounts for the film compositions we observe (Figures 1–3). Moreover, optical emission spectroscopy (OES) data of CW benzaldehyde plasmas in our laboratory show strong signals from both excited-state CO and α -H emission at all powers.²¹

Additional supporting evidence for processes such as Scheme 1 during plasma polymerization can be obtained from the work of Zhao et al.^{10,11} First, the CH aldehyde

bond is considered extremely labile,²² especially in plasmas,⁴ primarily because it is the weakest bond in benzaldehyde.¹² Second, complete conversion of aldehyde to ketone functional groups has been observed by Zhao et al. in the films produced by CW plasma polymerization of benzaldehyde.^{10,11} Finally, the neutral effluent from the benzaldehyde plasma using a hyphenated GC/MS technique showed significant generation of benzene, diphenyl ketone, and smaller unsaturated compounds at CW powers of 60 W.¹⁰ The authors proposed that the formation of diphenyl ketone



was through gas-phase reactions of benzoyl radicals (I) (Scheme 1), resulting in ketone functional groups in the deposited film. The formation of benzene results from cleavage of the C–C bond to the aldehyde, generating CO as a byproduct (Scheme 1). Production of CO was not confirmed by the GC/MS experiments of Zhao et al.,^{10,11} however, because they could only determine high-boiling point organic species.¹⁰ CO₂ was observed in pyrolysis of the films, further confirming the presence of ketone structures in the film. Further fragmentation results in the formation of acetylene.⁴ As noted above, we have independent support for the formation of gas-phase CO and H atoms (two byproducts of Scheme 1) from our OES data.²⁰ Additional support for the decarboxylation fragmentation pathway can be derived from our XPS data. Films deposited from low rf peak powers have high C/O ratios (Table 2), which indicate lower oxygen content, and this ratio decreases significantly when the peak power is increased to 50 W. This strongly suggests that oxygen is lost during the film formation process, presumably in the form of CO.

As shown in Figures 1 and 2, significant control can be exercised over film composition with pulsed plasmas through manipulation of pulse parameters and peak pulse power. For example, changing the applied peak pulse power from 25 to 50 W while keeping all other deposition conditions constant results in two completely different films. The film deposited at low peak power has a significant contribution from aromatic functional groups and has only ketone carbonyl moieties in the film (Figure 1). One possible explanation for this is preferential cleavage of the labile aldehyde CH bond, creating significant amounts of benzoyl radicals (I). These labile carbonyl species then react with incoming neutral molecules, causing fragmentation and deposition of a film with a high concentration of aromatic ketone structures.

In contrast, films deposited from the highest peak power plasmas have almost no aromatic retention (Tables 2 and 3) but do have aldehyde carbonyl moieties in the deposited film. At the higher powers there is more energy to cleave the aromatic ring, which can result in the generation of a diradical species, as proposed by Yasuda.⁴ This can be visualized in Scheme 2. Although Scheme 1 fragmentation pathways will still occur at high powers, the probability of other fragmen-

tation routes such as Scheme 2 also occurring is greater under these conditions. It should be noted that Scheme 2 results in the creation of gas-phase diradical species which are likely to play an influential role in any subsequent film growth steps. Polymerization reactions involving diradicals are not easily terminated,⁴ resulting in extensive chain propagation reactions that may preserve some of the aldehyde groups.²³ Thus, even though the fragmentation pathways shown in Schemes 1 and 2 can both occur at higher peak powers, formation of intermediates such as II (Scheme 2) offers pathways that favor aldehyde stability through resonance stabilization. Production of type II intermediates could account for the higher retention of aldehyde moieties seen under higher powers and lower pressures.

The system pressure affects the fragmentation pathways in a similar manner. When the reactor pressure is 25 mTorr (14/56 pulse cycle), there is little aromatic structure retained in the deposited film. The primary functional groups observed in the FTIR spectrum are from aldehyde carbonyls at 1701 cm⁻¹ and sp³ hybridized carbons at ~2950 cm⁻¹. As the pressure is increased to 100 mTorr using the same monomer flow rate and pulse sequence, the gas-phase species undergo more collisions and have a longer residence time in the reactor. There is, however, an effective decrease in the energy input per unit mass of monomer. The combination of increased residence time and decreased power/monomer results in decarboxylation but retention of the aromatic structure in the deposited film. This suggests the Scheme 1 fragmentation pathway is dominating the deposition process at higher system pressures. This is supported by the work of Zhao et al.^{10,11} who observed a similar change in film structure when the system pressure of a 20 W CW benzaldehyde plasma was increased from 20 to 50 mTorr.¹⁰ They reported an increase in aromatic retention at 50 mTorr but observed a concomitant decrease in the amount of hydroxyl groups in their films. There was, however, no aldehyde retention in any of their films. As a final note, hydroxyl groups in the bulk films (Figures 1–3), could likely result from a number of possible reaction pathways, including hydrogen atom reduction of carbonyls in the film, oxygen atom reactions with the film, and post-deposition reactions with atmospheric water.

The change in concentration of surface polar groups in our benzaldehyde pulsed-plasma-polymerized films can also be observed by the relative changes in the surface contact angle. Films deposited with 6 ms on times and 100 mTorr of operating pressure show no change in contact angle over the range of duty cycles employed (3–20%), within experimental error. This implies there is little change in the surface concentration of polar groups under these conditions. In contrast, contact angles for films deposited at lower pressures or longer on times show a significant dependence on plasma duty cycle (Figure 5). Higher duty cycles result in films with higher carbonyl moieties and, thus, higher surface polarity. Surface hydroxyls cannot account for the observed change in contact angle, as the TFAA derivatization experiments show a small, relatively constant amount of C–O–H surface groups in films deposited under different conditions (Table 3). Note that, with benzaldehyde, maximum retention of the aldehyde occurs at the highest duty cycle, whereas, with other monomers such as allyl alcohol,¹ acetonitrile, and acrylonitrile,²⁴ lower duty cycles result in maximum

retention of functional groups. As discussed above, this is explained by the different fragmentation pathways described in Schemes 1 and 2. It should also be noted that benzaldehyde fragmentation pathways involve aromatic-ring-opening processes while fragmentation of these other monomers involves cleavage of vinylic double bonds or triple bonds.

This work demonstrates that pulsed plasmas can afford unique film chemistries and greater control over film functional groups. Clearly more work is needed to explore alternate aldehyde monomers as well as subsequent chemical derivatization of functional groups introduced during plasma polymerization.²⁵ In addition, we plan to explore the effects of aging on the films produced from aldehyde monomers.

Acknowledgment. The authors gratefully acknowledge Prof. David G. Castner of the University of Washington for performing XPS analysis on our films. This work was supported by the National Science Foundation. M.A.L. also acknowledges support from the NSF-REU program.

References and Notes

- (1) Rinsch, C. L.; Chen, X.; Panchalingam, V.; Eberhart, R. C.; Wang, J.-H.; Timmons, R. B. *Langmuir* **1996**, *12*, 2995.
- (2) Savage, C. R.; Timmons, R. B.; Lin, J. W. In *Structure-Property Relations in Polymers*, Advances in Chemistry Series 236; American Chemical Society: Washington, DC, 1993; p 745.
- (3) Mackie, N. M.; Castner, D. G.; Fisher, E. R. *Langmuir* **1998**, *14*, 1227. Mackie, N. M.; Fisher, E. R. *Polym. Prepr.* **1997**, *38*, 1059.
- (4) Yasuda, H. *Plasma Polymerization*; Academic Press: Orlando, FL, 1985.
- (5) Mackie, N. M.; Dalleska, N. F.; Castner, D. G.; Fisher, E. R. *Chem. Mater.* **1997**, *9*, 349.
- (6) *Plasma Deposition, Treatment and Etching of Polymers*; d'Agostino, R., Ed.; Academic Press: Boston, 1990.
- (7) Panchalingam, V.; Chen, X.; Savage, C. R.; Timmons, R. B.; Eberhart, R. C. *J. Appl. Polym. Sci.: Appl. Polym. Symp.* **1994**, *54*, 123.
- (8) McCurdy, P. R.; Truitt, J. M.; Fisher, E. R. *J. Electrochem. Soc.* **1998**, *145*, 3271.
- (9) Beumer, G. J.; Gong, X.; Dai, L.; St. John, H. A. W.; Griesser, H. J. *Polym. Prepr.* **1997**, *38*, 1037.
- (10) Zhao, Q.; Zhu, Y.; Cai, M.; Xie, M.; Liu, X. *J. Appl. Polym. Sci.* **1992**, *45*, 110.
- (11) Zhao, Q.; Zhu, Y.; Xu, Y.; Yao, Y.; Liu, X. *J. Appl. Polym. Sci.* **1992**, *44*, 1853.
- (12) Calculated using the gas-phase thermochemistry found in: Lias, S. G.; Bartmess, J. E.; Liebman, J. F.; Holmes, J. L.; Levin, R. D.; Mallard, W. G. *J. Phys. Chem. Ref. Data* **1988**, *17*, Suppl. 1.
- (13) Bogart, K. H. A.; Dalleska, N. F.; Bogart, G. R.; Fisher, E. R. *J. Vac. Sci. Technol., A* **1995**, *13*, 476.
- (14) Rinsch, C. L.; Chen, X.; Panchalingam, V.; Eberhart, R. C.; Wang, J.; Timmons, R. B. *Langmuir* **1996**, *12*, 2995.
- (15) Colthup, N. B.; Daly, L. H.; Wiberley, S. E. *Introduction to Infrared and Raman Spectroscopy*, 3rd ed.; Academic Press: New York, 1990.
- (16) Dischler, B. In *Amorphous Hydrogenated Carbon Films*; Koidl, P.; Oelhafen, O., Eds.; Proc. E-MRS; 1987; Vol. 17, p 189.
- (17) Derivatization procedures were developed to minimize atmospheric exposure and crosscontamination of samples with TFAA, although trace amounts of TFAA adsorbed on our reactor after pumping to a base pressure of 3 mTorr may contribute to the trace F atom signal observed with XPS.
- (18) Beamson, G.; Briggs, D. *High-Resolution XPS of Organic Polymers, The Scienta ESCA 300 Database*; John Wiley and Sons: New York, 1992.
- (19) The large error bars on this figure are the result of difficulties with film delamination during the contact angle measurements.
- (20) Yasuda, H.; Hsu, T. *J. Polym. Sci., Polym. Chem. Ed.* **1977**, *14*, 81.
- (21) Emission corresponding to the $B^1\Sigma^+ - A^1\Pi$ transition of CO is observed at 450.93, 482.99, 519.07, and 519.56 nm and that corresponding to the $2p^2P^0 - 3d^2D$ H_α transition is at 656.2 nm. Harshbarger, W. R.; Porter, R. A.; Miller, T. A.; Norton, P. *Appl. Spectrosc.* **1977**, *31*, 201. Barshilia, H. C.; Mehta, B. R.; Vankar, V. D. *J. Mater. Res.* **1996**, *11*, 2852.
- (22) Morrison, R. T.; Boyd, R. N. *Organic Chemistry*, 4th ed.; Allyn and Bacon: Boston, 1983.
- (23) Flory, P. J. *Principles of Polymer Chemistry*; Cornell University Press: Ithaca, New York, 1953.
- (24) Lefohn, A. E.; Mackie, N. M.; Fisher, E. R. *Plasmas Polym.*, submitted for publication.
- (25) Williams, K. L.; Mackie, N. M.; Fisher, E. R. unpublished work.

MA980332C